Key Engineering Materials
ISSN: 1662-9795, Vol. 926, pp 1703-1712
doi:10.4028/p-qvfxm2

Submitted: 2021-12-01
Revised: 2022-02-08
Accepted: 2022-02-09
Online: 2022-07-22

Synthesis of ZnO and CuO Nanowires by Thermal Oxidation on Metallic Substrates

M.M. Arafat[1,a*], A.S.M.A. Haseeb[2,b], S. Rozali[3,c], D. Brabazon[4,d], B.M.A. Rahman[1,e], K.T.V. Grattan[1,f], S. Naher[1,g]

[1]School of Mathematics, Computer Science & Engineering, City, University of London, UK.

[2]Centre of Advanced Materials, Department of Mechanical Engineering, Faculty of Engineering, Universiti Malaya, Malaysia.

[3]Department of Mechanical Engineering, Faculty of Engineering, Universiti Malaya, Malaysia.

[4]School of Mechanical and Manufacturing Engineering, Dublin City University, Ireland.

[a]arafat.mahmood@city.ac.uk, arafat_mahmood@yahoo.com[a], [b]haseeb@um.edu.my, [c]azuar@um.edu.my, [d]dermot.brabazon@dcu.ie, [e]b.m.a.rahman@city.ac.uk, [f]k.t.v.grattan@city.ac.uk, [g]Sumsun.Naher.1@city.ac.uk

Keywords: 1D nanostructures, nanowires, thermal oxidation, ZnO, CuO.

Abstract. In this research work, brass (Cu - 37.2 wt% Zn) and Cu (99.9 wt%) wires having diameters of 200 μm were thermally oxidized in N_2 containing 5% O_2, at a flow rate of 200 sccm and in the ambient atmosphere respectively, to support the growth of nanowires. The oxidation temperature was varied from 300 to 600 °C and the as-grown nanowires were characterized by field emission scanning electron microscope (FESEM) equipped with energy dispersive X-ray (EDX) spectroscope, and transmission electron microscope (TEM). Results show that ZnO and CuO nanowires are formed on brass and Cu wires, respectively. The ZnO nanowires are branched and CuO nanowires are straight with tapered morphology. ZnO nanowires having hexagonal wurtzite structure grow along the <1 1 $\bar{2}$ 0> directions whereas, CuO nanowires have monoclinic structure. A diffusion based stress induced model is proposed to explain the growth mechanism of the nanowires. Thermal oxidation process is a suitable platform for synthesizing ZnO and CuO nanowires, which can be used in *in-situ* device fabrication.

Introduction

There is an ongoing interest in zinc oxide (ZnO) and cupric oxide (CuO) based semiconducting metal oxide nanostructures due to their unique electrical, chemical, magnetic, and optical properties. For example, ZnO is a *n*-type material that has a direct wide band gap of 3.37 eV at 300 K and large exciton binding energy of 60 meV [1-3]. Some of the opto-electronic and nano-electronic properties of ZnO overlap with GaN, which is another wide bandgap semiconductor (E_g ~3.4 eV at 300 K) possessing of attractive electrical, optical, and thermal properties [2, 4]. However, ZnO has some advantages over GaN, such as it has simpler routes for crystal growth and easy availability, which results in a lower cost of ZnO based devices [2]. On the other hand, CuO is a *p*-type material with narrow bandgap energy of 1.2 eV and conductivity of 10^{-7}-10^{-3} S.cm^{-1} [5, 6]. CuO is an anti-ferromagnetic material with a Néel temperature of 230 K, which exhibits super-thermal conductivity, photovoltaic properties, high stability, and antimicrobial activity [7]. These unique combinations of properties in ZnO and CuO based materials draw attention to the researchers and they have been extensively studied in light of their many potential engineering applications, such as UV laser [1], photo-detector [8, 9], field emitter [10, 11], gas sensor [12, 13], solder cell [14, 15], Li-ion battery [16, 17], supercapacitor [18, 19], and catalyst [20, 21]. For this reason, there is an ongoing effort to synthesize long, low-defect and highly crystalline ZnO and CuO nanowires at a lower cost.

In the recent years, a rich family of morphological variations of ZnO and CuO based nanostructures has been synthesized by various innovative techniques, such as hydrothermal [12,

22], electrospinning [23, 24], ultrasonic irradiation [25, 26], sol-gel [27, 28], chemical vapour deposition [20, 29], thermal evaporation [30, 31], pulsed laser deposition [32, 33], RF sputtering [34, 35], and molecular beam epitaxy [36, 37]. However, these methods often have associated problems including removal of catalyst and template, multi-steps and complex synthesis procedure, poor adhesion with underlying substrate, less scalability and expensive equipment [38]. Alternatively, thermal oxidation is a simple, single-step and inexpensive route for the formation of metal oxide nanostructures directly on metal substrates [38-42], which is desirable for many *in-situ* device fabrication processes [40]. In principle, nanowires of metal oxide based arrays synthesized by thermal oxidation can be electrically addressed by the supporting interdigitated electrodes for some applications, such as gas sensor and field emitter [40, 43, 44]. The resultant nanostructures obtained by thermal oxidation are highly crystalline and pure, which do not require any further treatment [38-42].

Due to engineering importance of ZnO and CuO nanostructures, recently combined effect of both ZnO and CuO nanostructures has been studied for various applications, including catalyst [45, 46], solar cell [47, 48], gas sensor [49], field emitter [50], and optoelectronics [51]. Promising results were obtained for the combined use of ZnO and CuO in the above mentioned applications [45-51]. Development of a simple, single step, scalable and catalyst-free platform for co-synthesising ZnO and CuO based nanostructures on metal substrates for the above mentioned applications will significantly reduce experimental complexity, time, and cost. Thermal oxidation can be an advantageous solution in these aspects.

In this research, thermal oxidation process is utilized for obtaining semiconducting one dimensional (1D) of ZnO and CuO nanowires on brass (Cu - 37.2 wt% Zn) and Cu (99.9%) wires, respectively. The oxidation temperature is optimized for the growth of nanowires. The nanowires and oxide layer beneath the nanowires are characterized by FESEM, EDX spectroscope, and TEM. Finally, a diffusion based stress induced mechanism is proposed for the growth of ZnO and CuO nanowires on brass and Cu substrates, respectively.

Experimental Procedure

As-received brass (Cu - 37.2 wt% Zn) and Cu (99.9%) wire having diameter of 200 μm was used in thermal oxidation. The experimental setup for thermal oxidation is described in the previous work [38]. In short, 5 cm long brass or Cu wire was placed in an alumina boat inside a horizontal tube furnace. The furnace was heated from ambient to 300-600 °C at a heating rate of 30 °C/min. The brass wire was oxidized in the presence of 5% O_2 in N_2 flown at a rate of 200 sccm, whereas the Cu wire was oxidized in ambient atmosphere. At the peak temperature, the wires were oxidized for 4 h. After 4 h of oxidation at the peak temperature, the furnace was switched off and cooled to room temperature by opening the lid of the furnace. The oxidation conditions of brass and Cu wire is presented in Table 1.

Table 1: Experimental conditions for the growth of nanowires on brass and Cu wires, respectively.

Substrate	*Oxidation temperature*	*Oxidation environment*	*Flow rate*	*Oxidation duration*
Brass (Cu - 37.2 wt% Zn) wire	300-600 °C	5% O_2 in N_2	200 sccm	4 h
Cu wire	300-600 °C	Ambient	-	4 h

The oxidized brass and Cu wires were characterized by FESEM equipped with EDX spectroscope. InLens detector was used in FESEM for the observation of oxidized surface. EDX spot analysis, line scan and elemental mapping were performed on the nanowires and the oxide scales beneath the nanowires. The nanowires were also observed under a high resolution transmission electron microscope (HRTEM: FEI Tecnai F-20). For this, oxidized brass wire was taken in a small bottle followed by the addition of 2.5 ml deionized water. Then the bottle was

ultrasonicated for 30 sec to scale off the nanowires. A tiny amount of the suspension was dropped on Cu grid using a micro-pipette followed by drying in oven at 60 °C for 1 h. Then the Cu grid was placed inside the HRTEM chamber for the high resolution observation of the oxides. The selected area diffraction (SAD) pattern was obtained from fast Fourier transformation (FFT).

Results and Discussion

Brass (Cu - 37.2 wt% Zn) wires were oxidized in the presence of 5% O_2 in N_2 at a flow rate of 200 sccm at temperatures ranging from 300 to 600 °C for 4 h. After oxidation, the brass wires became greyish in colour.

The FESEM images of brass wires after 4 h of oxidation at different temperatures are shown in Fig. 1. For oxidation temperatures of 300 °C, short and inconsistent forms of one dimensional (1D) nanostructures are seen (Fig. 1(a)). With increasing oxidation temperature to 350 °C, the length (1-2 μm) and coverage of the nanowires are increased (Fig. 1(b)) [38]. At oxidation temperature of 400 °C, combination of long and short nanowires is seen (Fig. 1(c)) [38]. The length of long nanowires is up to 6 μm from the root to the tip. For the oxidation temperature of 450 °C, high coverage of long nanowires with thin and thick morphologies is seen all over the brass wire (Fig. 1(d)) [38]. The diameter of thin nanowires is 50-200 nm with length of up to 30 μm. On the other hand, the diameter and length of thick nanowires is 200-500 nm and 5-15 μm, respectively with faceted morphology. Further increase in temperature to 500 °C, the nanostructures become shorter and the oxide scale exfoliates from the core of brass wire (Fig. 1(e)) [38]. This could be due to the reason that the α-β' phases in brass (Cu - 37.2 wt% Zn) transforms to α-β at 458 °C [52]. The transformation of β' to β may attributes to the growth of shorter nanowires at 500 °C [38]. The huge difference in a-axis thermal expansion coefficient of brass (19×10^{-6} K^{-1}) and ZnO (2.9×10^{-6} K^{-1}) is the reason for the exfoliation of oxide layers during cooling from 500 °C [38]. Beside this, the nanostructures transform to flat-cone shaped morphology at 500 °C [38]. Increasing temperature up to 600 °C, the length and coverage of the nanowires start increasing (Fig. 1(f) and 1(g)) [38]. So, from the results it is clear that 450 °C is the optimum temperature for the growth of nanowires on brass wire during thermal oxidation.

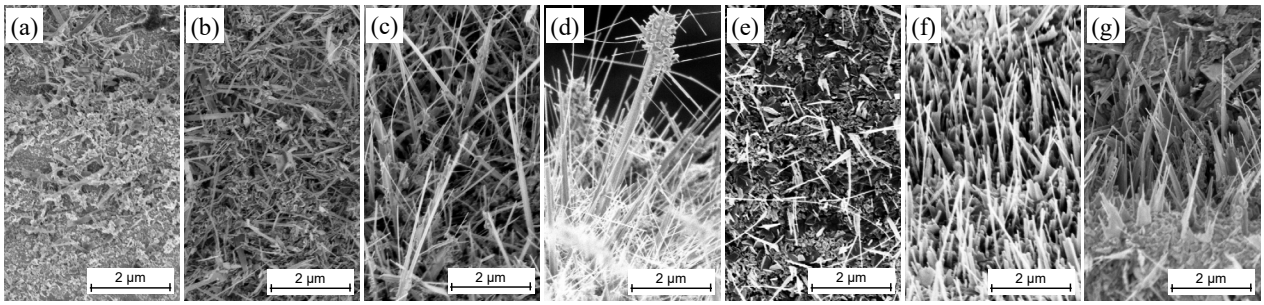

Fig. 1: FESEM images of brass (Cu - 37.2 wt% Zn) wires oxidized in the presence of 5% O_2 in N_2 flown at a rate of 200 sccm at temperatures of (a) 300 °C, (b) 350 °C, (c) 400 °C,(d) 450 °C, (e) 500 °C, (f) 550 °C, and (g) 600 °C.

Branching of nanowires is seen during oxidation of brass wire, prominently at 450 °C as seen in Fig. 2(a). The branches are originated from the irregularly shaped particles deposited on the top and side walls of thick nanowires. The length of the branches is 1-3 μm. In all cases, the branches are aligned at 60° angle with the main stem of the nanowires. Tough some branches in Fig. 2(a) appear to be perpendicular to the main stem, basically they are originated at 60° angle with the main stem. The angles of branches would be obvious when they are observed from correct perspectives. Some sort of entanglement is also observed in branches, which could be due to the presence of defect sites. The elemental mapping of the nanowires is shown in Fig. 2(b-d) and the presence of Zn and O is obvious (Fig. 2(b, c)), which confirms that the nanowires are ZnO. The presence of Cu is also observed in the elemental mapping (Fig. 2(d)). It is expected that some Cu in the form of CuO is present in nanowires. However, further studies are required to confirm the CuO doping in ZnO nanowires.

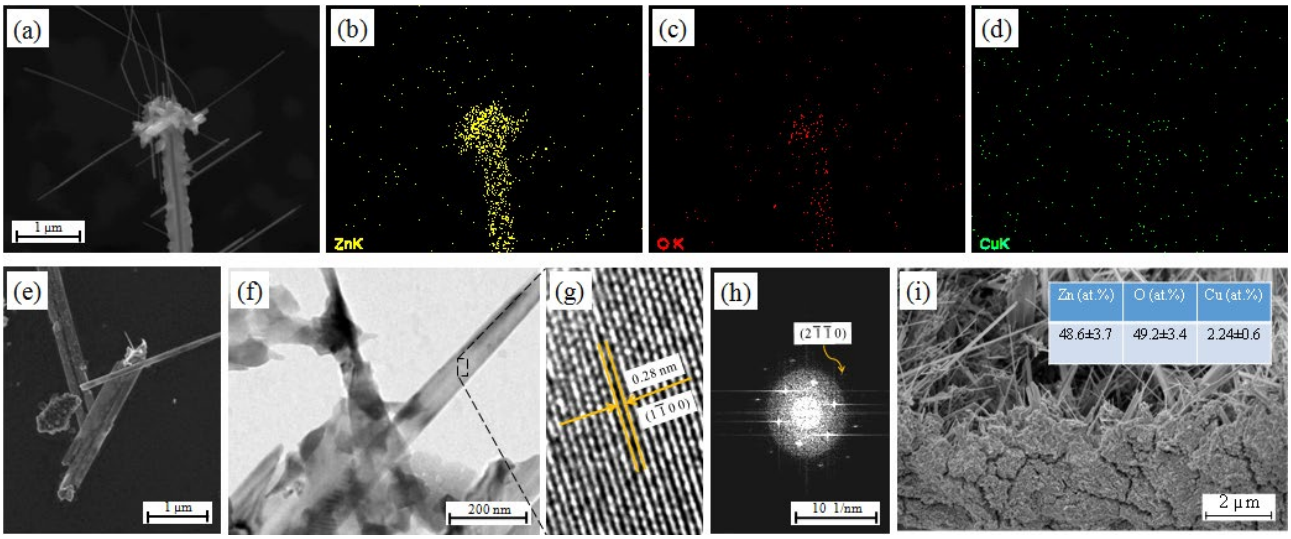

Fig. 2: (a) FESEM image of branched ZnO nanowires grown at 450 °C, (b-d) corresponding EDX spectroscope elemental mapping of Zn, O and Cu, respectively, (e) FESEM images of thick nanowires on TEM grid, (f) bright-field TEM image of thin nanowires, (g) corresponding HRTEM image, (h)corresponding SAD pattern, and (i) exfoiled oxidzed layer in cross-sectional view and corresponding EDX spot analysis of the oxidized layer (inset).

The ZnO nanowires were observed under a TEM. To prepare the samples, the ZnO nanowires were taken on Cu TEM grid and observed under FESEM as seen in Fig. 2(e) followed by observation under HRTEM. It appears from Fig. 2(e) that the thick ZnO nanowires are consist of a few thin nanowires. Probably during oxidation at higher temperatures they fused together due to the diffusion of atoms. Fig. 2(f) shows the bright-field TEM image of ZnO nanowires having a thickness of 50 nm. The HRTEM image of the main stem of the nanowires shows the (1 $\bar{1}$0 0) crystal planes of hexagonal wurtzite ZnO (Fig. 2(g)). The SAD pattern focusing on the main stem confirms that the ZnO nanowires grow along the [2 $\bar{1}$ $\bar{1}$ 0] directions (Fig. 2(h)). In our previous study, we have confirmed that the branches of the ZnO nanowires grow along the [1 1 $\bar{2}$ 0] direction [38]. It should be noted that [2 $\bar{1}$ $\bar{1}$ 0] and [1 1 $\bar{2}$ 0] is the same family of direction and are angled at 60° with each other. So, it is clear that the ZnO nanowires and its branches grows along the <1 1 $\bar{2}$ 0> directions.

The FESEM image of the exfoiled oxidized layer on brass wire is shown in Fig. 2(i) in cross-section. The EDX spectroscope spot analysis is performed on the oxide layer beneath the ZnO nanowires. The EDX spectroscope analysis confirms that the oxide layer is ZnO with some Cu content (~2 at%). It is expected that during oxidation, Cu also migrates to the surface together with Zn and reacts with oxygen to form CuO.

The growth mechanism ZnO nanowires on brass (Cu - 37.2 wt% Zn) substrate was proposed in our previous work [38]. As the liquidous temperature of brass alloy containing 37.2 wt% Zn is significantly higher (~900 °C) compared to the oxidation temperature, it is expected that no melting is involved in the present case [38]. So, vapour-liquid-solid (VLS) or vapour-solid (VS) mechanism is not applicable for the growth of ZnO nanowires on brass substrate as explained by others for the growth of ZnO nanowires on pure Zn substrates [53-55]. According to the proposed mechanism, the Zn atoms migrate towards the surface of brass wire to form ZnO layer and as a result the surface becomes Zn rich [38]. The crystallographic structure of ZnO is hexagonal wurtzite and brass (Cu-37.2 wt% Zn) is a solid solution of face centred cubic and body centred cubic structures. It is expected that a compressive stress is generated at the oxide-metal interface due to the mismatches in volume, density and crystallographic structures of ZnO layer and brass substrate [38]. This compressive stress is released by forming new surfaces in the form of ZnO nanowires on the ZnO layer during oxidation [56]. The side-walls of ZnO nanowires are facing to (0 0 0 1) planes, which is favourable for transporting of Zn atoms from the root to the tip of the nanowires [44]. Zn atoms at

the tip of the nanowires react with oxygen for further growth of the nanowires. It should be noted that the vapour pressure of Zn (0.491 mbar) is significantly higher than Cu ($3.12x10^{-15}$ mbar) at 450 °C [57]. So, it is expected that some fraction of diffused Zn vaporized and reacts with oxygen to form ZnO, which deposits on the family of <1 1 $\bar{2}$ 0> crystal planes of the growing ZnO nanowires (Fig. 2(a)). Stress is accumulated at the nucleation sites and relaxed by forming branches of ZnO nanowires. The <1 1 $\bar{2}$ 0> crystal planes are angled at 60° with each other and for this reason the branches are aligned at 60° with the main stem of the ZnO nanowires. Little amount of Cu is also diffused to the surface during oxidation and it is expected that the ZnO nanowires are doped with CuO. However, further studies are required to confirm this fact.

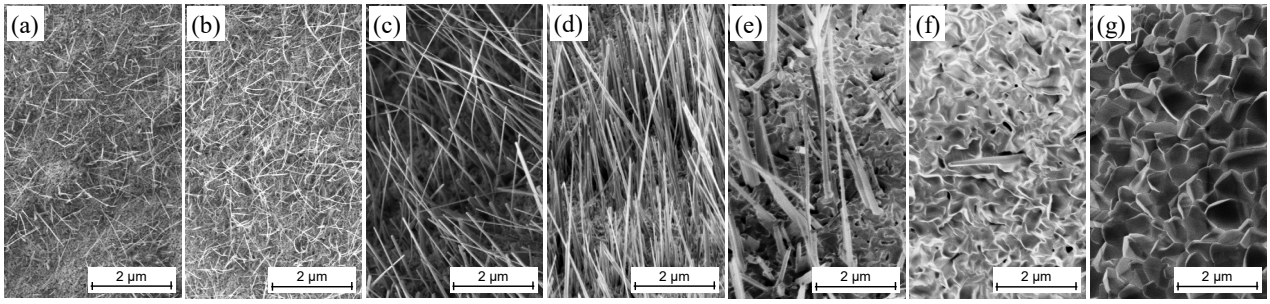

Fig. 3: FESEM images of Cu wires oxidized in ambient at temperatures of (a) 300 °C, (b) 350 °C, (c) 400 °C,(d) 450 °C, (e) 500 °C, (f) 550 °C, and (g) 600 °C.

The Cu wires were also oxidized at 300-600 °C in the ambient. After oxidation Cu wires turned to black colour. Fig. 3 shows the oxidized surface of Cu wires at different oxidation temperatures. Low coverages of nanowires are seen at the oxidation temperature of 300 °C (Fig. 3(a)). With increasing the temperatures until 450 °C, the diameter, length, and coverage of the nanowires are increased as seen in Fig. 3(b-d). At temperature of 450 °C, nanowires having length up to 10 µm is seen with daimeter of 80-200 nm. At 500 °C, the coverage of nanowires is decreased (Fig. 3(e)). Beyond 500 °C, oxide scale is observed (Fig. 3(f) and Fig. 3(g)). From the results, 450 °C is considered the optimum temperature for the growth of nanowires on Cu wire.

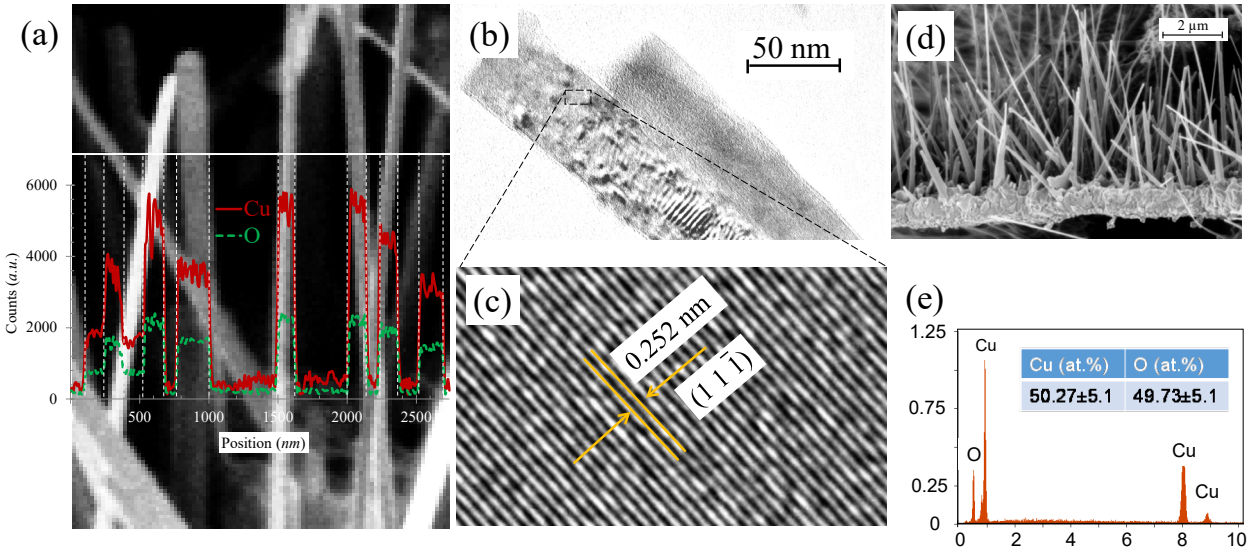

Fig. 4: (a) FESEM image of CuO nanowires grown at 450 °C and corresponding elemental line scanning, (b, c) bright-field TEM image of nanowires and corresponding HRTEM image, (d, e) exfoiled oxidzed layer in cross-sectional view and corresponding EDX spot analysis.

Fig. 4(a) shows the FESEM images of few nanowires and corresponding line scanning. The nanowires are straight with no branching. Beside this, the nanowires are slightly tapered from the bottom to the tip. The presence of Cu and O is confirmed from the line scanning and thus it is concluded that the nanowires are CuO. Fig. 4(b) shows the bright-field TEM image of CuO

nanowires and the corresponding HRTEM image is shown in Fig. 4(c). The HRTEM image shows the (1 1 $\bar{1}$) crystal planes of monoclinic CuO (Fig. 4(c)). The FESEM image of exfoiled oxidized layer of Cu wire is shown in Fig. 4(d) and the corresponding EDX spectroscope spot analysis in Fig. 4(e). It is confirmed from the atomic ratios in EDX spectroscope analysis that oxide layer beneath the CuO nanowires is also CuO. However, in the literature formation of Cu_2O is observed beneath the CuO layer [58, 59], which was not peeled off during exfoilation in the present case. So, the configuration of Cu wire after oxidation from outermost interface to innermost interface is as follows: CuO nanowires - CuO layer - Cu_2O layer - Cu core.

Previously, stress induced mechanism was proposed by Kumar *et al*. [56] to explain the growth of CuO nanowires on Cu substrate by thermal oxidation. During oxidation, CuO nanowires grows directly on intermediate CuO layer, which grows on inner Cu_2O layer [58, 59]. At the initial stage of oxidation, Cu atoms reacts with the oxygen and CuO layer is formed at the surface. At the later stage, Cu^{2+} ions diffuse to the surface through the grain boundaries and O^{2-} counter diffuse [59-62] and as a result Cu_2O layer is formed beneath the CuO layer. The formation of simple cubic Cu_2O underneath monoclinic CuO layer during oxidation induces a substantial stress at the interface, which is relaxed by forming CuO nanowires [56]. Diffusion of oxygen from outer surface to the interface of CuO/Cu_2O layers also accumulates stress, which favors the growth of nanowires [56]. The grain boundary runs along the entire length of the nanowires and acts as a path for short-circuit diffusion transport of Cu ions to the tip for the growth of nanowires [60].

Table 2: Summary of thermal oxidation process and characterizations of brass and Cu wires.

Criterion	*Parameter*	*Brass (Cu - 37.2 wt% Zn) wire*	*Cu wire*
Process parameter	Optimum oxidation temperature	450 °C	450 °C
	Oxidation environment	5% O_2 in N_2 flown at a rate of 200 sccm	Ambient
Characterization	Composition	ZnO. The nanowires may bedoped with CuO. Further studies are required.	CuO
	Morphology	Thin and thick nanowires with branchs. At oxidation temperatures of ≥500 °C, flat-cone shaped morphology is seen.	Straight nanowires with slightly tappered morphology.
	Diameter and length (at oxiation temperature of 450 °C)	Diameter: 50-500 nm Length: up to 30 µm	Diameter: 80-200 nm Length: up to 10 µm
	Crystal structure	Wurtzite	Monoclinic
	Growth direction	<1 1 $\bar{2}$ 0>	-
	Oxide layer beneath the nanowires	ZnO	CuO and Cu_2O
Growth mechanism	-	Diffusion based stress induced mechanism	Diffusion based stress induced mechanism

Table 2 summarizes the growth of ZnO and CuO nanowires on brass and Cu wires during thermal oxidation, respectively. Both of the nanowires optimally grow at 450 °C in a single experimental setup. As both ZnO and CuO nanowires have engineering importance and in many instances, they are used combinedly for various applications, including catalyst [45, 46], solar cell [47, 48], gas sensors [49], field emitter [50], and optoelectronics [51], the thermal oxidation process could be a lucrative approach for the growth of 1D ZnO and CuO nanowires. Beside, this process provides an easy, inexpensive, and highly scalable platform for the growth of these nanowires. In addition, this method also facilitates the growth of nanowires directly on the substrate, making it particularly suitable for many *in-situ* device fabrication processes, including gas sensors and field emitters [40, 43, 44].

Conclusions

In this work, brass (Cu - 37.2 wt% Zn) and Cu wires were oxidized for the growth of nanowires. The nanowires and the oxide scale beneath the nanowires were characterized. The key findings of the research can be summarized as shown below:

- ZnO are formed on brass wire during thermal oxidation in the presence of 5% O_2 in N_2 flown at a rate of 200 sccm at 450 °C. The nanowires may be doped with CuO. Further studies are required to confirm this fact. On the other hand, CuO nanowires are formed on Cu wires during thermal oxidation in ambient at 450 °C.
- ZnO nanowires have thin and thick morphologies with branches. The diameter of the ZnO nanowires is 50-500 nm and lengths up to 30 μm. The branches are 1-3 μm long. On the other hand, CuO nanowires are straight with slightly tapered morphology. The diameter of the CuO nanowires is 80-200 nm and lengths up to 10 μm.
- ZnO nanowires having hexagonal wurtzite structure grow along the <1 1 $\bar{2}$ 0> directions. The CuO nanowires have monoclinic structure.
- ZnO layer is formed beneath the ZnO nanowires during the oxidation of brass substrates. On the other hand, CuO and Cu_2O layers are formed beneath the CuO nanowires during the oxidation of Cu substrates.
- A diffusion-based stress induced model is proposed to explain the mechanism of ZnO and CuO nanowires growth on brass and Cu substrates, respectively.

Acknowledgement

This project is funded by European Commission under Marie Skłodowska-Curie Actions (MSCA) Individual Fellowships scheme (Project No.: 898736), with additional financial support provided by City, University of London institutional grant (University Research Pump-Priming Fund).

References

[1] M.H. Huang, S. Mao, H. Feick, H. Yan, Y. Wu, H. Kind, E. Weber, R. Russo, P. Yang, Room-temperature ultraviolet nanowire nanolasers, Science. 292 (2001) 1897-1899.

[2] Ü. Özgür, Y.I. Alivov, C. Liu, A. Teke, M.A. Reshchikov, S. Doğan, V. Avrutin, S.-J. Cho, H. Morkoç, A comprehensive review of ZnO materials and devices, J. Appl. Phys. 98 (2005) 041301.

[3] D.C. Look, B. Claflin, Y.I. Alivov, S.J. Park, The future of ZnO light emitters, Phys. Status Solidi A. 10 (2004) 2203-2212.

[4] M. Xiao, Comparative optical spectroscopy of gallium-nitride and aluminum-nitride nanostructures deposited onto silicon substrate, Optik. 127 (2016) 4396-4399.

[5] S.B. Wang, C.H. Hsiao, S.J. Chang, K.T. Lam, K.H. Wen, S.C. Hung, S.J. Young, B.R. Huang, A CuO nanowire infrared photodetector, Sens. Actuator A Phys. 171 (2011) 207-211.

[6] S. Mridha, D. Basak, Investigation of a p-CuO/n-ZnO thin film heterojunction for H_2 gas-sensor applications, Semicond. Sci. Technol. 21 (2006) 928-932.

[7] A. Zúñiga, L. Fonseca, J.A. Souza, C. Rivaldo-Gomez, C.D. Pomar, D. Criado, Anomalous ferromagnetic behavior and size effects in CuO nanowires, J. Magn. Magn. Mater. 471 (2019) 77-81.

[8] R. Khan, P. Uthirakumar, T.H. Kim, I.-H. Lee, Enhanced photocurrent performance of partially decorated Au nanoparticles on ZnO nanorods based UV photodetector, Mater. Res. Bull. 115 (2019) 176-181.

[9] M. Tetseo, P. Deb, S. Daimary, J.C. Dhar, CuO nanowire-based metal semiconductor metal infrared photodetector, Appl. Phys. A. 127 (2021) 380.

[10] L. Wang, Y. Zhao, K. Zheng, J. She, S. Deng, N. Xu, J. Chen, Fabrication of large-area ZnO nanowire field emitter arrays by thermal oxidation for high-current application, Appl. Surf. Sci. 484 (2019) 966-974.

[11] H.T. Hsueh, T.J. Hsueh, S.J. Chang, T.Y. Tsai, F.Y. Hung, S.P. Chang, W.Y. Weng, B.T. Dai, CuO-nanowire field emitter prepared on glass substrate, IEEE Trans. Nanotechnol. 10 (2011) 1161-1165.

[12] R. Gao, X. Cheng, S. Gao, X. Zhang, Y. Xu, H. Zhao, L. Huo, Highly selective detection of saturated vapors of abused drugs by ZnO nanorod bundles gas sensor, Appl. Surf. Sci. 485 (2019) 266-273.

[13] S. Kulkarni, R. Ghosh, A simple approach for sensing and accurate prediction of multiple organic vapors by sensors based on CuO nanowires, Sens. Actuators B Chem. 335 (2021) 129701.

[14] M.I. Fathima, K.S.J. Wilson, Role of multilayer antireflective coating in ZnO based dye sensitized solar cell, Vacuum. 165 (2019) 58-61.

[15] M. Iqbal, A. A.Thebo, A.H. Shah, A. Iqbal, K. H.Thebo, S.Phulpoto, M.A. Mohsin, Influence of Mn-doping on the photocatalytic and solar cell efficiency of CuO nanowires, Inorg. Chem. Commun. 76 (2017) 71-76.

[16] Y. Ding, J. Xu, L. Chen, J. Yao, S. Dai, J. Wu, T. Hayat, A. Alsaedi, Pierced ZnO nanosheets via a template-free photopolymerization in microemulsion, J. Alloys Compd. 787 (2019) 779-785.

[17] L.B. Chen, N. Lu, C.M. Xu, H.C. Yu, T.H. Wang, Electrochemical performance of polycrystalline CuO nanowires as anode material for Li ion batteries, Electrochim. Acta. 54 (2009) 4198-4201.

[18] Q. Luo, P. Xu, Y. Qiu, Z. Cheng, X. Chang, H. Fan, Synthesis of ZnO tetrapods for high-performance supercapacitor applications, Mater. Lett. 198 (2017) 192-195.

[19] X. Zhang, C. Zhang, A. Abas, Y. Zhang, X. Mu, J. Zhou, Q. Su, W. Lan, E. Xie, Ag nanoparticles enhanced vertically-aligned CuO nanowire arrays grown on Cu foam for stable hybrid supercapacitors with high energy density, Electrochim. Acta. 296 (2019) 535-544.

[20] J.L. Yang, S.J. An, W.I. Park, G.-C. Yi, W. Choi, Photocatalysis using ZnO thin films and nanoneedles grown by metal-organic chemical vapor deposition, Adv. Mater. 16 (2004) 1661-1664.

[21] N. Kana, K. Kaviyarasu, T. Khamliche, C.M. Magdalane, M. Maaza, Stability and thermal conductivity of CuO nanowire for catalyticapplications, J. Environ. Chem. Eng. 7 (2019) 1032552.

[22] M.E. Bustos, F. Hevia, S. Fuentes, A.I. Martínez, R.A. Zárate, A novel route for the preparation of self-assembled CuO hierarchical nanostructures by hydrothermal processing at high pressure, Mater. Lett. 297 (2021) 129936.

[23] K.-S. Choi, S.-P. Chang, Effect of structure morphologies on hydrogen gas sensing by ZnO nanotubes, Mater. Lett. 230 (2018) 48-52.

[24] H. Guan, C. Shao, B. Chen, J. Gong, X. Yang, A novel method for making CuO superfine fibres via an electrospinning technique, Inorg. Chem. Commun. 6 (2003) 1409-1411.

[25] E. Oh, H.-Y. Choi, S.-H. Jung, S. Cho, J.C. Kim, K.-H. Lee, S.-W. Kang, J. Kim, J.-Y. Yun, S.-H. Jeong, High-performance NO_2 gas sensor based on ZnO nanorod grown by ultrasonic irradiation, Sens. Actuators B Chem. 141 (2009) 239-243.

[26] S.M.K. Aboul-Fotouh, Methanol conversion to DME as a blue fuel: The beneficial use of ultrasonic irradiation for the preparation of CuO/H-MOR nanocatalyst, J. Fuel Chem. Technol. 42 (2014) 1340-1350.

[27] S. Delice, M. Isik, N.M. Gasanly, Traps distribution in sol-gel synthesized ZnO nanoparticles, Mater. Lett. 245 (2019) 103-105.

[28] N. Kumar, S.S. Parui, S. Limbu, D.K. Mahato, N. Tiwari, R.N. Chauhan, Structural and optical properties of sol-gel derived CuO and Cu_2O nanoparticles, Mater. Today: Proc. 41 (2021) 237-241.

[29] N. Chen, F. Ju, F. Zhou, S. Chen, K. Wei, P. He, Growth and characterization of chemical vapor deposition diamond coating incorporated amorphous carbon with high Raman bands induced by CuO particles, Diam. Relat. Mater. 116 (2021) 108387.

[30] S.Y. Bae, C.W. Na, J.H. Kang, J. Park, Comparative structure and optical properties of Ga-, In-, and Sn-doped ZnO nanowires synthesized via thermal evaporation, J. Phys. Chem. B. 109 (2005) 2526-2531.

[31] D. Mahana, A.K. Mauraya, P. Pal, P. Singh, S.K. Muthusamy, Comparative study on surface states and CO gas sensing characteristics of CuO thin films synthesised by vacuum evaporation and sputtering processes, Mater. Res. Bull. 145 (2022) 111567.

[32] C.-Q. Luo, F.C.-C. Ling, M.A. Rahman, M. Phillips, C. Ton-That, C. Liao, K. Shih, J. Lin, H.W. Tam, A.B. Djurišić, S.-P. Wang, Surface polarity control in ZnO films deposited by pulsed laser deposition, Appl. Surf. Sci. 483 (2019) 1129-1135.

[33] A.A. Menazea, A.M. Mostafa, Ag doped CuO thin film prepared via pulsed laser deposition for 4-nitrophenol degradation, J. Environ. Chem. Eng. 8 (2020) 104104.

[34] A.Z. Sadek, S. Choopun, W. Wlodarski, S.J. Ippolito, K. Kalantar-zadeh, Characterization of ZnO nanobelt-based gas sensor for H_2, NO_2, and hydrocarbon sensing, IEEE Sens.J. 7 (2007) 919-924.

[35] J.L.S. Cuaila, A.M.H.d. Andrade, J. Geshev, M. Gamino, Correlations between parameters and structure of CuO(111) films grown by RF reactive sputtering at room temperature, Mater. Today: Pro. 14 (2019) 164-167.

[36] H.T. Wang, B.S. Kang, F. Ren, L.C. Tien, P.W. Sadik, D.P. Norton, S.J. Pearton, J. Lin, Hydrogen-selective sensing at room temperature with ZnO nanorods, Appl. Phys. Lett. 86 (2005) 243503.

[37] K.G. Yang, P. Hu, S.X. Wu, L.Z. Ren, M. Yang, W.Q. Zhou, F.M. Yu, Y.J. Wang, M. Meng, G.L. Wang, S.W. Li, Room-temperature ferromagnetic CuO thin film grown by plasma-assisted molecular beam epitaxy, Mater. Lett. 166 (2016) 23-25.

[38] M.M. Arafat, S. Rozali, A.S.M.A. Haseeb, S. Ibrahim, Direct and catalyst-free synthesis of ZnO nanowires on brass by thermal oxidation, Nanotechnology. 31 (2020) 175603.

[39] M.M. Arafat, B. Dinan, A.S.M.A. Haseeb, S.A. Akbar, B.M.A. Rahman, S. Rozali, S. Naher, Growth of 1D TiO_2 nanostructures on Ti substrates incorporated with residual stress through humid oxidation and their characterizations Nanotechnology. 32 (2021) 475607 (475617pp).

[40] M.M. Arafat, A.S.M.A. Haseeb, S.A. Akbar, M.Z. Quadir, In-situ fabricated gas sensors based on one dimensional core-shell TiO_2-Al_2O_3 nanostructures, Sens. Actuators B Chem. 238 (2017) 972-984.

[41] M.M. Arafat, A.S.M.A. Haseeb, S.A. Akbar, Growth and characterization of the oxide scales and core/shell nanowires on Ti-6Al-4V particles during thermal oxidation, Ceram. Int. 41 (2015) 4401-4409.

[42] M.M. Arafat, A.S.M.A. Haseeb, B. Dinan, S.A. Akbar, Stress enhanced TiO_2 nanowire growth on Ti-6Al-4V particles by thermal oxidation, Ceram. Int. 39 (2013) 6517-6526.

[43] K. Huo, Y. Hu, J. Fu, X. Wang, P.K. Chu, Z. Hu, Y. Chen, Direct and large-area growth of one-dimensional ZnO nanostructures from and on a brass substrate, J. Phys. Chem. C. 111 (2007) 5876-5881.

[44] X. Wen, Y. Fang, Q. Pang, C. Yang, J. Wang, W. Ge, K.S. Wong, S. Yang, ZnO nanobelt arrays grown directly from and on zinc substrates: synthesis, characterization, and applications, J. Phys. Chem. B. 109 (2005) 15303-15308.

[45] S. Likhittaphon, R. Panyadee, W. Fakyam, S. Charojrochkul, T. Sornchamni, N. Laosiripojana, S. Assabumrungrat, P. Kim-Lohsoontorn, Effect of CuO/ZnO catalyst preparation condition on alcohol-assisted methanol synthesis from carbon dioxide and hydrogen, Int. J. Hydrog. Energy. 44 (2019) 20782-20791.

[46] C.-M. Chou, Y.-C. Chang, P.-S. Lin, F.-K. Liu, Growth of Cu-doped ZnO nanowires or ZnO-CuO nanowires on the same brass foil with high performance photocatalytic activity and stability, Mater. Chem. Phys. 201 (2017) 18-25.

[47] S. Paul, J. Sultana, A. Karmakar, S. Chattopadhyay, Effect of prolonged growth on the chemical bath deposited ZnO nanowires and consequent photovoltaic performance of n-ZnO NWs/p-CuO heterojunction solar cells, Mater. Today: Proc. 4 (2017) 12496-12499.

[48] J. Sultana, S. Paul, R. Saha, S. Sikdar, A. Karmakar, S. Chattopadhyay, Optical and electronic properties of chemical bath deposited p-CuO and n-ZnO nanowires on silicon substrates: p-CuO/n-ZnO nanowires solar cells with high open-circuit voltage and short-circuit current, Thin Solid Films. 699 (2020) 137861.

[49] Y.H. Navale, S.T. Navale, F.J. Stadler, N.S. Ramgir, V.B. Patil, Enhanced NO_2 sensing aptness of ZnO nanowire/CuO nanoparticle heterostructure-based gas sensors, Ceram. Int. 45 (2019) 1513-1522.

[50] L. Sun, E. Chen, T. Guo, Field emission enhancement of composite structure of ZnO quantum dots and CuO nanowires by Al_2O_3 transition layer optimization, Ceram. Int. 46 (2020) 15565-15571.

[51] M.A. Khan, N. Nayan, M.K. Ahmad, S.C. Fhong, M.S.M. Ali, M.K. Mustafa, M. Tahir, Interface study of hybrid CuO nanoparticles embedded ZnO nanowires heterojunction synthesized by controlled vapor deposition approach for optoelectronic devices, Opt. Mater. 117 (2021) 111132.

[52] T. B. Massalski (Editor-in-Chief), H. Okamoto, P.R. Subramanian, L. Kacprzak (Editors), Binary alloy phase diagrams, 2nd edition, ASM International, Materials Park, Ohio, USA, (1990).

[53] M.R. Khanlary, V. Vahedi, A. Reyhani, Synthesis and characterization of ZnO nanowires by thermal oxidation of Zn thin films at various temperatures, Molecules. 17 (2012) 5021-5029.

[54] O. Martíneza, V. Hortelano, J. Jiménez, J.L. Plaza, S.d. Dios, J. Olvera, E. Diéguez, R. Fath, J.G. Lozano, T. Ben, D. González, J. Mass, Growth of ZnO nanowires through thermal oxidation of metallic zinc films on CdTe substrates, J. Alloys Compd. 509 (2011) 5400-5407.

[55] H.-Q. Liang, L.-Z. Pan, Z.-J. Liu, Synthesis and photoluminescence properties of ZnO nanowires and nanorods by thermal oxidation of Zn precursors, Mater. Lett. 62 (2008) 1797-1800.

[56] A. Kumar, A.K. Srivastava, P. Tiwari, R.V. Nandedkar, The effect of growth parameters on the aspect ratio and number density of CuO nanorods, J. Phys. Condens. Matter. 16 (2004) 8531-8543.

[57] Information on https://www.iap.tuwien.ac.at/www/surface/vapor_pressure (accessed on 25 November 2021).

[58] J. Liang, N. Kishi, T. Soga, T. Jimbo, Cross-sectional characterization of cupric oxide nanowires grown by thermal oxidation of copper foils, Appl. Surf. Sci. 257 (2010) 62-66.

[59] L. Yuan, Y. Wang, R. Mema, G. Zhou, Driving force and growth mechanism for spontaneous oxide nanowire formation during the thermal oxidation of metals, Acta Mater. 59 (2011) 2491-2500.

[60] B.J. Hansen, G. Lu, J. Chen, Direct oxidation growth of CuO nanowires from copper-containing substrates, J. Nanomater. 2008 (2008) Article ID: 830474.

[61] F. Wu, Y. Myung, P. Banerjee, Unravelling transient phases during thermal oxidation of copper for dense CuO nanowire growth, CrystEngComm. 16 (2014) 3264-3267.

[62] A.M.B. Gonçalves, L.C. Campos, A.S. Ferlauto, R.G. Lacerda, On the growth and electrical characterization of CuO nanowires by thermal oxidation, J. Appl. Phys. 106 (2009) 034303.